EVALUATION OF DATA FROM EXPERIMENTS WITH SPARK AND LASER GENERATED BUBBLES

K. Vokurka*)

Faculty of Electrical Engineering, Czech Technical University, Suchbátarova 2, 166 27 Praha 6, Czechoslovakia

Experimental data on spark and laser generated bubbles published in the literature are evaluated and compared with a theoretical model. It is found that within the first bubble oscillation the theory agrees rather well with the experiments. However, for later oscillations unaccounted energy losses occur in real bubbles. These losses seem to be of the same origin as the losses discussed in connection with explosion generated bubbles.

1. INTRODUCTION

Due to the random nature of cavitation, direct observation of cavitation bubbles is extremely difficult. Therefore, in experiments, the cavitation bubbles are often substituted by spark and laser generated bubbles. Over the years a number of experimental results on the spark and laser generated bubbles have accumulated in the literature. The results have usually been interpreted directly by the authors themselves, but there is a lack of a unifying approach that would interpret all these experiments from the same viewpoint.

In this work we want to fill this gap to some extent. The published experimental data will be evaluated by means of a method recently presented in reference [1], and the results will be compared with a theoretical model given in a previous paper [2]. Suitable criteria allowing discrimination between gas and vapour bubbles in experiments will also be postulated.

Throughout this work the same notation as that introduced in a closely related paper [2] is used. Hence, as the reader is assumed to be familiar with this previous work, not all the symbols will be defined here again.

2. EXPERIMENTAL TECHNIQUES

Before starting to evaluate the experimental data it may be useful to review briefly the details of the techniques used to generate spark and laser bubbles.

2.1. Spark generated bubbles

In a spark test two electrodes are submerged in a liquid and a capacitor is discharged via a conducting channel formed between them. The passage of an intense current

*) Present address: *Department of Research and Development, LIAZ, o.p., V. Kopeckého 400, 466 05 Jablonec n. N., Czechoslovakia.*

pulse through the channel causes local overheating accompanied by an evaporation and a subsequent dissociation and ionization of the liquid molecules and atoms [3, 4].

Depending upon the experimental arrangement, the plasma in the channel is heated to temperature s ranging from 15 000 K to 30 000 K and the pressures attained are of the order 100 MPa [3, 4]. The current pulse typically lasts 10 – 100 μs, and the energy released may be as high as 100 kJ [4].

After the discharge has been initiated a shock wave is emitted. At the same time the channel starts expanding and forms a vapour bubble that performs several damped oscillations. As the peak pressure in the shock wave is approximately two orders lower than in the case of underwater explosions the shock wave is relatively weak (for example, Shima et al. [5] measured an initial shock velocity $U = 1950\ \mathrm{m\ s^{-1}}$, which corresponds to the shock pressure of 500 MPa [6]). The vapour bubble, on the other hand, oscillates very violently and emits bubble pulses much stronger than those emitted by the explosion generated bubbles.

Though it is difficult to assign any precise physical meaning to such quantities as "the bubble initial radius R_{m0}", "the initial pressure P_{M0}", and "the polytropic exponent γ" (the bubble starts growing from almost zero volume and the energy supply lasts a relatively long time), these quantities do represent convenient parameters enabling one to use a simple computational model introduced in reference [2]. And, as will be shown later, this model, in spite of its simplicity, gives meaningful results which reflect real conditions rather well.

2.2. Laser generated bubbles

When an intense laser pulse is focused into a liquid the light is partially absorbed on impurities present in the focal point (another hypothesis regarding the initiation of the process assumes a breakdown of the liquid resulting from the high intensity of the electromagnetic field in the focal point). Due to the local increase in the concentration of heat a portion of the liquid surrounding the impurities is converted into vapour and plasma at high pressure and temperature. The violent increase in the pressure results in emission of a shock wave and a subsequent expansion of an overheated vapour nucleus [7, 8]. The vapour bubble thus generated performs several oscillations during which strong bubble pulses are emitted [7, 9 – 12].

Though the laser pulse has a finite duration (usually of the order 10^{-8} s [7 – 12]), to simplify the analysis it will be assumed again that a time $t = 0$ a spherical bubble with an initial radius R_{m0}, filled with vapour at pressure P_{M0} and temperature Θ_{M0}, is formed in the liquid. The initial vapour temperature was measured by Barnes and Rieckhoff [13] to be $\Theta_{M0} = 15\,000$ K. However, no direct data concerning the initial pressure P_{M0} are available.

Nevertheless the value of the pressure P_{M0} can be estimated indirectly from comparison of the waveforms emitted during the spark and laser tests. If we denote the peak pressures in the shock and in the first bubble pulse as p_{p0} and p_{p1} respectively

[2], then, for example, in the case of the spark tests it usually holds that $p_{p0} < p_{p1}$ (see, e.g., fig. 1.2 in reference [4], fig. 9a in reference [14], and fig. 3 in reference [15]). On the other hand, in the case of the laser tests it usually holds that $p_{p0} > p_{p1}$ (see, e.g., fig. 4 in reference [7] and fig. 2 in reference [11]; however, this need not be always true as is proved by fig. 2 in reference [12]). If one assumes that the bubble collapse mechanisms for the two techniques are the same, then the pressure P_{M1} should also be the same (cf. table 2 in reference [2]). Therefore it can be concluded that the initial pressures P_{M0} generated by lasers are usually higher than the initial pressures generated by discharges. Specifically, from the comparison of the ratios p_{p0}/p_{p1} in the two cases and from what is known about P_{M0} in the case of the spark tests it can be estimated that in the laser tests $P_{M0} = 0{\cdot}5 - 1$ GPa.

3. EVALUATION OF EXPERIMENTAL DATA

The bubble behaviour can be studied in a number of ways; with a hydrophone [7, 9–11, 14, 15], by high-speed cinematography [16, 17], or high-speed holo-cinematography [18], by streaking and framing schlieren photographs [5], and several others. In this section we want to evaluate some of the experimental data and compare them with theoretical results from reference [2].

3.1. Peak pressure data

The variation of the peak pressure in the first bubble pulse, p_{p1}, with the bubble size, R_{M1}, was measured by several researchers. For example, Mellen [14] studied spark generated bubbles, and as shown in reference [19] his data can be fitted by two curves

$$p_{p1} = 3{\cdot}87 \times 10^{10} R_{M1}^{2{\cdot}7}\ [\mathrm{Pa, m}]\,, \quad R_{M1} \in (6;\ 10{\cdot}8)\ [\mathrm{mm}]\,, \tag{1}$$

$$p_{p1} = 1{\cdot}67 \times 10^{7} R_{M1}\ [\mathrm{Pa, m}]\,, \quad R_{M1} \in (10{\cdot}8;\ 27)\ [\mathrm{mm}]\,. \tag{2}$$

The measurements were done at a distance $r = 1$ m from the bubble center and at an ambient pressure $p_\infty = 100$ kPa. After substituting relations (1), (2) into the definition formula for the position independent acoustic pressure p_{zp1}($p_{zp1} = p_{p1} r/(p_\infty R_{M1})$ [20]) one obtains

$$p_{zp1} = 3{\cdot}87 \times 10^{5} R_{M1}^{1{\cdot}7}\ [\mathrm{m}]\,, \quad R_{M1} \in (6;\ 10{\cdot}8)\ [\mathrm{mm}]\,, \tag{3}$$

$$p_{zp1} = 167\,, \quad R_{M1} \in (10{\cdot}8;\ 27)\ [\mathrm{mm}]\,. \tag{4}$$

Beside the spark generated bubbles Mellen [14] has also studied bubbles generated by exploding wires. According to his measurements no noticeable difference in the value of p_{p1} was registered in the two tests. This is an interesting result, as one would rather expect that due to the presence of the evaporated metal in the bubble interior the oscillations would be less violent.

Another measurement of the bubble pulse peak pressure was reported by Teslenko [9, 10], who worked with laser generated bubbles. His data (fig. 3 in reference [9] and fig. 2 in reference [10]) can be fitted by a curve

(5) $$p_{p1} = 3{\cdot}08 \times 10^9 R_{M1}^{1.25}\ [\text{Pa, m}]\,, \quad R_{M1} \in (1; 5)\ [\text{mm}]\,.$$

For this case $r = 15$ mm and $p_\infty = 100$ kPa, so one obtains

(6) $$p_{zp1} = 462 R_{M1}^{0.25}\ [\text{m}]\,, \quad R_{M1} \in (1; 5)\ [\text{mm}]\,.$$

Similar measurements with laser generated bubbles were also reported by Hentschel and Lauterborn [11]. These authors determined that (fig. 4 in reference [11])

(7) $$p_{p1} = 3{\cdot}95 \times 10^{12} R_{M1}^{2.5}\ [\text{Pa, m}]\,, \quad R_{M1} \in (2{\cdot}2; 4)\ [\text{mm}]\,.$$

As in this case $r = 10$ mm and $p_\infty = 100$ kPa, one obtains

(8) $$p_{zp1} = 3{\cdot}95 \times 10^5 R_{M1}^{1.5}\ [\text{m}]\,, \quad R_{M1} \in (2{\cdot}2; 4)\ [\text{mm}]\,.$$

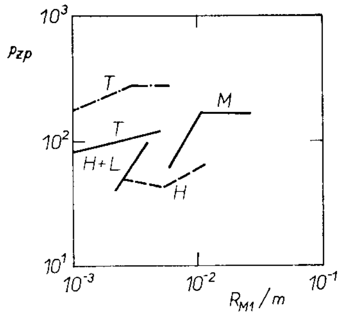

Fig. 1. Variation of the first bubble pulse peak pressure, p_{zp1}, with the bubble size, R_{M1}. The sources of the experimental data: ——— T — Teslenko [9], fig. 3, and [10], fig. 2; ——— H + L — Hentschel and Lauterborn [11], fig. 4; ——— M — Mellen [14], fig. 12; —·—·—·— T — Teslenko [22], fig. 4b; — — — — H — Harrison [24], fig. 11.

Eqs. (3), (4), (6), and (8) are displayed in fig. 1. Though the peak pressures, p_{zp1}, measured by different researchers show vast scatter, they do have one common feature: for the bubble sizes ranging from $R_{M1} = 1$ mm to $R_{M1} = 10{\cdot}8$ mm it holds that with an increase in R_{M1} the peak pressure p_{zp1} also increases and that for $R_{M1} > 10{\cdot}8$ mm the peak pressure p_{zp1} is constant, i.e. independent of R_{M1}. Such behaviour can be explained by the presence of heat losses for bubbles smaller than $R_{M1} = 10{\cdot}8$ mm and by the absence of size-dependent effects for bubbles larger than $R_{M1} = 10{\cdot}8$ mm [19].

As can be seen, only Mellen [14] studied the scaling bubbles (i.e., the bubbles with $R_{M1} > 10{\cdot}8$ mm [19]). Using his value of the peak pressure, $p_{zp1} = 167$, the amplitude of the scaling bubbles oscillations was determined in references [1, 21] to be $A_1 = 3{\cdot}29$ if $\gamma = 1{\cdot}25$ and $A_1 = 3{\cdot}5$ if $\gamma = 1{\cdot}33$.

The difference in the slope and in the absolute value of the peak pressure curves in fig. 1 is most probably due to the different physical conditions (such as the concentration of the dissolved gases and impurities in water, water temperature, etc.), and to the different experimental arrangements. However, further experiments are urgently needed to throw more light on this problem.

Let us note that despite the vast scatter among the data from different sources, the peak pressures measured during one experimental series usually show a relatively high correlation and that the data from different series are approximately of the same order, which only further indicates that the values of the amplitudes $A_1 = 3{\cdot}3$ and $A_1 = 3{\cdot}5$ are quite correct.

Teslenko [22] has also studied variation of the peak pressure in the shock wave, p_{p0}, with the bubble size, R_{M1} (fig. 4b in reference [22]). His data can be fitted by two curves

$$p_{p0} = 1{\cdot}72 \times 10^{10} R_{M1}^{1.385} \;[\text{Pa, m}]\,, \quad R_{M1} \in (1; 3)\;[\text{mm}]\,, \tag{9}$$

$$p_{p0} = 1{\cdot}83 \times 10^{9} R_{M1} \;[\text{Pa, m}]\,, \quad R_{M1} \in (3; 6)\;[\text{mm}]\,. \tag{10}$$

As in this case $r = 15$ mm and $p_\infty = 100$ kPa, one has

$$p_{zp0} = 2{\cdot}58 \times 10^{3} R_{M1}^{0.385} \;[\text{m}]\,, \quad R_{M1} \in (1; 3)\;[\text{mm}]\,, \tag{11}$$

$$p_{zp0} = 275\,, \quad R_{M1} \in (3; 6)\;[\text{mm}]\,. \tag{12}$$

Eqs. (11) and (12) are displayed in fig. 1 by chain lines. It can be seen that for the bubble sizes $R_{M1} > 3$ mm the quantities p_{zp0} and R_{M1} are mutually independent.

Eq. (12) can be used to estimate the value of the initial pressure, P_{M0}. This can be conveniently done in the expansion W system of variables. If we assume that $W_{M1} = 20-30$ (see table I in reference [2]), then we obtain that $p_{wp0} = p_{zp0} W_{M1} = 5\,500-8\,250$. If we further assume that the shock wave is propagated as an acoustic wave along most of its path (see, e.g., figs. 5 and 6 in reference [7], and fig. 5 in reference [23]), then the pressure p_{wp0} is approximately equal to the initial pressure P^*_{M0} ($P^*_{M0} = p_{wp0} + 1$ [20]).

Measurements of p_{p1} vs. R_{M1} were also reported by Harrison [24] and Chahine et al. [15]. Harrison used an exploding wire technique and his results (fig. 11 in reference [24]) can be fitted by two curves

$$p_{p1} = 1{\cdot}98 \times 10^{7} R_{M1}^{0.84} \;[\text{Pa, m}]\,, \quad R_{M1} \in (2{\cdot}5; 5{\cdot}6)\;[\text{mm}]\,, \tag{13}$$

$$p_{p1} = 7{\cdot}34 \times 10^{8} R_{M1}^{1.54} \;[\text{Pa, m}]\,, \quad R_{M1} \in (5{\cdot}6; 11{\cdot}4)\;[\text{mm}]\,. \tag{14}$$

As now $r = 0{\cdot}1$ m and $p_\infty = 100$ kPa, one obtains

$$p_{zp1} = 19{\cdot}8 R_{M1}^{-0.16} \;[\text{m}]\,, \quad R_{M1} \in (2{\cdot}5; 5{\cdot}6)\;[\text{mm}]\,, \tag{15}$$

$$p_{zp1} = 734 R_{M1}^{0.54} \;[\text{m}]\,, \quad R_{M1} \in (5{\cdot}6; 11{\cdot}4)\;[\text{mm}]\,. \tag{16}$$

Eqs. (15) and (16) are displayed in fig. 1 by the dashed lines. Because the slope of the curves (15) and (16) differs substantially from other results these measurements have been mentioned only after discussion of other data.

Finally, Chahine et al. [15] found that $p_{p1} \sim R_{M1}^{1.5}$ (fig. 6 in reference [15]). Hence $p_{zp1} \sim R_{M1}^{0.5}$. However, as the authors do not give the appropriate units of the variables in their graph, it is not possible to display these data in fig. 1.

3.2. Damping factor data

The damping factor, $\alpha_1 = R_{M2}/R_{M1}$, represents another quantity that can yield valuable information on the bubble behaviour. It is also a quantity that can be most often determined from the published data, be it either the bubble radius vs. time curves or the radiated pressure vs. time records. In the latter case the quantity which is being determined is $\beta_1 = T_{02}/T_{01}$, where T_{01} and T_{02} are the times of the first and second bubble oscillations, respectively. As shown in reference [1] for the case of the gas bubbles, β_1 is always larger than α_1, but the actual difference is small (typically $\alpha_1/\beta_1 = 0.98$). Though no similar study has been conducted in the case of vapour bubbles, in what follows we shall assume that $\alpha_1 \doteq \beta_1$.

Hentschel and Lauterborn give measured variation of R_{M2} with R_{M1} (fig. 3 in reference [11]) for laser generated bubbles. Their data can be fitted by a straight line, the slope of which directly equals the damping factor, α_1. Thus in this case it can be determined that $\alpha_1 = 0.5 \pm 0.05$. An interesting feature to be seen in fig. 3 in reference [11] is that for the given bubble-size range, i.e. for $R_{M1} = 1-5$ mm, the damping factor is bubble-size independent.

Shima and Tomita [17] give a graph (fig. 8 in reference [17]), from which it immediately follows that the value of the damping factor α_1 in their measurements was between 0.3 and 0.62. The authors do not explicitly mention the bubble sizes for which α_1 was determined, but if one assumes that the data given in fig. 7 in reference [17] stem from the same group of bubbles, then the bubble sizes R_{M1} range from 2 to 15 mm. Though no conclusion as to the variation of α_1 with R_{M1} can be drawn from reference [17], we shall assume that, as in the data of Hentschel and Lauterborn [11], α_1, here, is also bubble-size independent.

The data of Hentschel and Lauterborn [11] and Shima and Tomita [17] are displayed together with some other experimental data in fig. 2. From fig. 2 it follows that the average value of the experimental damping factor is approximately $0.45-0.5$ and that the individual data seem to support the assumption regarding the independence of α_1 from R_{M1}. Note also the relatively large scatter of α_1 (not only within the measurements of Shima and Tomita [17]).

On the assumption that the amplitude of the bubble oscillations, A_1, can be correctly determined from the value of the peak pressure, p_{zp1}, it was found in reference [1] that for the scaling spark generated bubbles and $\gamma = 1.25$ the corresponding amplitude is $A_1 = 3.29$ and that for $\gamma = 1.33$ it is $A_1 = 3.5$. By means of a bubble model based on the assumption that the only dissipative mechanism present in the scaling bubbles is the acoustic radiation, the independent functions $\alpha = \alpha(A, \gamma)$ were computed in reference [1]. From these functions we can determine that for the gas bubbles, oscillating with the amplitudes mentioned, the theoretical damping factors are $\alpha_1 = 0{\cdot}73$ (for $A_1 = 3{\cdot}29$ and $\gamma = 1{\cdot}25$) and $\alpha_1 = 0{\cdot}72$ (for $A_1 = 3{\cdot}5$ and $\gamma = 1{\cdot}33$). For the vapour bubbles the necessary data are given in table 1 in reference [2], from which it follows that $\alpha_1 = 0{\cdot}71$ ($A_1 = 3{\cdot}29, \gamma = 1{\cdot}25$).

When comparing these damping factors with the data given in fig. 2 it can be seen that the theoretical values of α_1 are much larger than the experimental ones. An obvious explanation for this discrepancy is the existence of a dissipative mechanism that was not taken into account in the theoretical model. Let us note that a similar discrepancy was also encountered when evaluating data originating in underwater explosion research [1, 27]. In that case the theoretical damping factor was $\alpha_1 = 0{\cdot}85$ ($A_1 = 2{\cdot}05, \gamma = 1{\cdot}25, p_\infty = 1{\cdot}62$ MPa) but the experimental one was $\alpha_1 = 0{\cdot}68$.

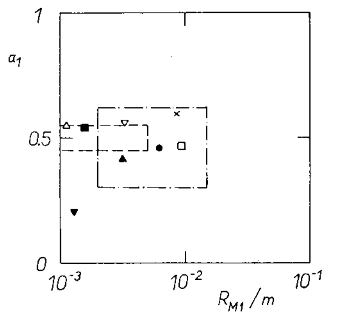

Fig. 2. Variation of the damping factor, α_1, with the bubble size, R_{M1}. The sources of the experimental data: — — — — Hentschel and Lauterborn [11], fig. 3; —•— Shima and Tomita [17], fig. 8; △ — Shima and Tomita [17], fig. 9; ▲ — Shima and Tomita [17], fig. 12; ■ — Lauterborn [16], fig. 3; ▽ — Lauterborn [16], fig. 9; ▼ — Lauterborn [26], fig. 3; ● — Buzukov et al. [7] (data given in the text); × — Harrison [24], fig. 10; □ — Benkovskii et al. [25] (data given in the text).

Possible candidates for the unknown dissipative mechanism were also mentioned in reference [27]. These include: (a) turbulence in the surrounding liquid, (b) loss of the gas from the main bubble in the form of microbubbles, (c) cooling of the gas in protuberances, and (d) internal converging shocks. It is highly probable that the dissipative mechanism acting in the explosion generated bubbles is also responsible for the extra energy losses in the case of the spark and laser generated bubbles.

However, if we assume for a moment that the theoretical model given in reference [1] is correct, i.e. that the acoustic radiation is the only damping mechanism for the scaling bubbles, then we can use the independent functions $\alpha = \alpha(A, \gamma)$ (fig. 8 in reference [1]) to determine the amplitudes corresponding to the measured α_1. We shall find that, for $\alpha_1 = 0{\cdot}62$ and $\gamma = 1{\cdot}25$, for example, the amplitude is $A_1 = 4{\cdot}0$ and that for $\alpha_1 = 0{\cdot}62$ and $\gamma = 1{\cdot}33$ it is $A_1 = 4{\cdot}2$. However, for $\alpha_1 = 0{\cdot}3$ we obtain $A_1 = 8{\cdot}6$ ($\gamma = 1{\cdot}25$) and $A_1 = 9{\cdot}2$ ($\gamma = 1{\cdot}33$).

In our opinion, which is strongly supported by the measured peak pressure values in the bubble pulses (see, e.g., fig. 1) and by further evidence to be given in section 3.3, the amplitudes determined in such a way are highly exaggerated and the amplitudes determined from p_{zp1} are much more realistic (even if not necessarily completely correct).

Another interesting conclusion which can be drawn from fig. 2 concerns the variation of α_1 with R_{M1}. If one denotes the total energy dissipated between R_{M1} and R_{M2} as ΔE_d, then for the bubble sizes, R_{M1}, ranging from 1 to 10 mm one can write (in the Z system) [20]

$$\Delta E_{zd} = \Delta E_{za} + \Delta E_{zh} + \Delta E_{zu} . \tag{17}$$

Here ΔE_{za} is the radiated acoustic energy, ΔE_{zh} denotes heat losses from the bubble, and ΔE_{zu} all the remaining energy losses. For sufficiently intensive bubble oscillations the total dissipated energy approximately equals [1]

$$\Delta E_{zd} \doteq 1 - \alpha_1^3 . \tag{18}$$

As mentioned above, the data given in fig. 2 seem to suggest that α_1 is bubble-size independent. Then from (18) it follows that ΔE_{zd} does not change with R_{M1} either. However, it was shown in section 2.2 that in the given bubble-size range the quantity p_{zp1} increases with R_{M1} (fig. 1), and hence ΔE_{za} should also be increasing with R_{M1}. On the other hand, ΔE_{zh} should decrease with R_{M1} [19]. Nothing can be said at present about the variation of ΔE_{zu} with R_{M1}. However, the postulated bubble-size independence of α_1 suggests that the three dissipative terms act in such a way as to compensate each other, so that the average dissipated energy ΔE_{zd} remains constant for any bubble size.

3.3 Various data

An interesting series of optical measurements has recently been reported by Shima et al. [5] and Shima and Tomita [17]. For example, Shima et al. [5] determined the velocities of the first bubble pulse propagation in the liquid near the spark bubble wall. The measured initial velocities reached Mach numbers $M = c/c_\infty = 1{\cdot}25 - 1{\cdot}31$ (fig. 13 in reference [5]). From the Tait equation of state for water, the velocity of the pressure disturbances, P, at the bubble wall equals [1]

$$C = c_\infty[(P + B)/(p_\infty + B)]^{(n-1)/(2n)} , \tag{19}$$

where B and n are liquid constants. From eq. (19) one easily obtains

$$P = (p_\infty + B)\,(C/c_\infty)^{2n/(n-1)} - B . \tag{20}$$

After substituting the values of the constants B and n for water, i.e. $B = 300$ MPa and $n = 7$, the ambient pressure $p_\infty = 100$ kPa, and the measured Mach numbers into eq. (20), one finds that $P^*_{M1} = 2051 - 2635$. This pressure is of the same order as was computed using the theoretical model ($P^*_{M1} = 5460$ [2]). The difference between the theoretical and experimental values can be attributed to the presence of heat losses in the experimental bubbles.

Another interesting result reported in reference [5] is a measured maximum bubble wall velocity, $\dot{R}_{max} = 250$ m s^{-1}. Using the independent functions, $\dot{Z}_{max} = \dot{Z}_{max}(A, \gamma)$, given in reference [1] it is possible to determine that $A_1 = 2{\cdot}92$ ($\gamma = 1{\cdot}25$) and $A_1 = 3{\cdot}13$ ($\gamma = 1{\cdot}33$). These amplitudes are slightly lower than those determined from p_{zp1} in the case of the scaling bubbles. However, like in the preceding example, the difference can be explained by heat losses.

In a second study [17], using high-speed cinematography, Shima and Tomita followed the spark bubble behaviour for relatively long time intervals (spanning several bubble oscillations), and thus they were able to determine the residual radii, R_r, that were asymptotically approached by the bubbles at later stages. The residual bubbles are apparently filled with a non-condensable gas that, to some extent, has been present in the bubble since the discharge, and, to some extent, has diffused into the bubble interior during the oscillations. For bubble sizes $R_{M1} = 2-15$ mm, the authors determined that $R_r/R_{M1} = 0{\cdot}12-0{\cdot}31$ (fig. 7 in reference [17]).

Shima and Tomita assume that the majority of the gas has been present in the bubble since the discharge and treat the bubble as a pure gas bubble, i.e., they put $R_r = R_e$, and use the value of R_e thus obtained in determining the intensity of the bubble oscillations. Hence they find that $A_1 = R_{M1}/R_r = 3{\cdot}2-8{\cdot}3$.

Though the lower limit agrees with the estimates given in this work rather well, in our opinion such an interpretation of the residual radius R_r is not valid. As shown in reference [28] no gas bubble can be excited to oscillate in the expansion system with an amplitude larger than $A_1 \doteq 2{\cdot}5$. On the other hand, we believe that the spark bubbles are basically vapour bubbles, for which the intensity of the first oscillation is first of all determined by the collapse effect [21]. However, the data of Shima and Tomita [17] are highly valuable in assessing the amount of non-condensable gas entering the spark bubble interior through various mechanisms.

Finally, the results displayed in figs. 10 and 11 in reference [17] make it possible to determine the average damping factors even for later oscillations. Thus from the data given in fig. 10 in reference [17] it follows that $\alpha_1 = 0{\cdot}56$, $\alpha_2 = 0{\cdot}63$, $\alpha_3 = 0{\cdot}83$, and $\alpha_4 = 0{\cdot}94$ ($R_{M1} = 4{\cdot}5$ mm). Similarly, fig. 11 shows that $\alpha_1 = 0{\cdot}63$, and $\alpha_2 = 0{\cdot}71$ ($R_{M1} = 4{\cdot}5$ mm). These data also indicate the increasing amount of gas that has diffused into the bubble. Let us note, however, that as the bubbles were generated near a solid boundary, the oscillations were not as violent as if the bubbles had occurred far from the solid boundaries.

4. DISCUSSION

The mathematical model of the spark and laser generated bubbles introduced in reference [2] seems to be valid only for the first oscillation. At later stages a difference between computed and measured data occurs. This difference was attributed to a dissipative mechanism whose character is not yet fully understood.

All the experimental data discussed in this paper indicate that within the first bubble oscillation the calculated values are not too far from the actual ones. However, further experiments are needed to verify and explain some points. For example, Hentschel and Lauterborn [11] determined a relatively low scatter in the damping factor data ($\alpha_1 = 0{\cdot}5 \pm 0{\cdot}05$), whereas Shima and Tomita [17] determined a large one ($\alpha_1 = 0{\cdot}45 \pm 0{\cdot}15$). Another question to be verified concerns the variation of α_1 with R_{M1}. The data of Hentschel and Lauterborn [11] suggest that α_1 is independent of R_{M1} even for the non-scaling bubbles. Is this of general validity or restricted to particular conditions?

Yet another important question concerns the existence of the different exponents and factors in analytical curves used to fit the experimental data in the graphs p_{p1} vs. R_{M1}. It would also be very interesting to verify whether p_{zp1} really is functionally independent of R_{M1} for $R_{M1} > 10$ mm, and if so, for what range of bubble sizes (in theory, the peak pressure p_{zp1} should decrease again with increasing R_{M1} for macrobubbles [19]), and how this limiting value of R_{M1} depends on the experimental arrangement. In this respect we know only of the measurement performed by Mellen [14] and this is certainly too little to enable us to form any general conclusions. Another question still to be answered concerns the nature and value of the unknown energy, ΔE_u, and its variation with R_{M1}.

Though mathematical analysis presented in reference [2] is based on the scaling bubbles, to date most experiments have been performed with bubbles for which thermal conduction is important. Hence inclusion of heat losses into the existing model is essential for further progress.

Though, as a rule, during the violent bubble oscillations instabilities develop in the wall motion, in none of the references cited here have the authors reported any observations of a complete breakup of the spark and laser generated bubbles upon their collapse (only Harrison [24] observed complete bubble breakups; however, it was in connection with venturi nozzle cavitation bubbles). Thus it seems highly probable that bubbles oscillating with amplitudes $A_1 < 3{\cdot}5$, unless influenced by external forces, do not disintegrate completely during their lives.

The pressure waves radiated upon bubble collapses are often referred to as shock waves (see, e.g. references [5, 10, 11]). However, the experimental pressure vs. time records published up to the present do not allow us to judge whether the shock has really developed in the leading edge of the bubble pulse along its initial propagation path. The only fact which is known is that soon after leaving the bubble wall the pulse is already propagated with a sonic velocity [5]. Thus it is most probable that even if the shock develops in the liquid near the minimum radius, it quickly degenerates and is propagated further as an ordinary acoustic wave.

It was experimentally determined that the damping factor of bubbles produced by underwater explosions equals approximately $\alpha_1 \doteq 0{\cdot}7$ [1]. As it is most probable that no other gas bubble can be excited in the expansion system to oscillate more violently than the explosion generated bubble, then this value of α_1 represents a certain limit, which can be used to discriminate between the vapour and gas bubbles: if $\alpha_1 \geqq 0{\cdot}7$, the bubble is filled with a gas, and if $\alpha_1 < 0{\cdot}7$, the bubble is filled with a vapour. Let us remind that typical values of α_1 for the spark and laser generated bubbles lie between 0·3 and 0·6. In our opinion this discrimination rule can most probably be used even in connection with other excitation techniques (due to the collapse effect [21] the damping factor of the vapour bubbles should be independent of the excitation technique), but further research is certainly needed to validify this hypothesis.

Another possible discrimination rule suggested in reference [2] is based on the mutual relation between p_{p0} and p_{p1}. For example, it was shown that the relation $p_{p0} < p_{p1}$ is possible only for vapour bubbles [2]. Hence, in view of this, the bubbles produced by Popov and Kogarko [29] are typical vapour bubbles (this also follows directly from the composition of the original explosive gaseous mixture: $2\,H_2 + O_2$) and the observed "unusual" pressure waveforms and bubble radius vs. time histories are not due to heat losses as suggested by the authors, but due to the specific behaviour of the vapour bubbles.

It is difficult to estimate at present how far the results obtained here (e.g., the value of P^*_{M1}) are transferable to cavitation bubbles. Let us only note that the results presented are significantly lower than the values sometimes given in the literature (see, e.g., table 4-4 in reference [30]).

Received 21. 11. 1986.

References

[1] Vokurka K.: Czech. J. Phys. B *36* (1986) 600.
[2] Vokurka K.: Czech. J. Phys. B *38* (1988) 27.
[3] Martin E. A.: J. Appl. Phys. *31* (1960) 255.
[4] Naugolnykh K. A., Roi N. A.: Electrical Discharges in Water. Nauka, Moscow, 1971 (in Russian).
[5] Shima A., Takayama K., Tomita Y., Miura N.: Acustica *48* (1981) 293.
[6] Cole R. H.: Underwater Explosions. Princeton University Press, Princeton, 1948.
[7] Buzukov A. A., Popov Yu. A., Teslenko V. S.: Zh. Prikl. Mekh. & Tekh. Fiz. No. 5 (1969) 17.
[8] Felix M. P., Ellis A. T.: Appl. Phys. Lett. *19* (1971) 484.
[9] Teslenko V. S.: Zh. Prikl. Mekh. & Tekh. Fiz. No. 4 (1976) 109.
[10] Teslenko V. S.: *in* Cavitation and Inhomogeneities in Underwater Acoustics (ed. W. Lauterborn). Springer, Berlin, 1980, p. 30.
[11] Hentschel W., Lauterborn W.: Appl. Sci. Res. *38* (1982) 225.
[12] Schmidt-Kloiber H., Reichel E.: Acustica *54* (1984) 284.
[13] Barnes P. A., Rieckhoff K. E.: Appl. Phys. Lett. *13* (1968) 282.
[14] Mellen R. H.: J. Acoust. Soc. Am. *28* (1956) 447.
[15] Chahine G. L., Courbiere P., Garnaud P.: *in* Proceedings of the 6th Conference on Fluid Machinery (eds. Kisbocskói L., Szabó Á.). Akademiai Kiado, Budapest, 1979, Vol. 1, p. 200.
[16] Lauterborn W.: Acustica *31* (1974) 51.
[17] Shima A., Tomita Y.: Ing.-Arch. *51* (1981) 243.
[18] Lauterborn W., Hentschel W.: Ultrasonics *23* (1985) 260.

[19] Vokurka K.: Acustica *60* (1986) 269.
[20] Vokurka K.: Czech. J. Phys. B *35* (1985) 28, 110, 121.
[21] Vokurka K.: J. Acoust. Soc. Am. *81* (1987) 58.
[22] Teslenko V. S.: Kvantovaya Elektron. *4* (1977) 1732.
[23] Bjørnø L.: Trans. ASME J. Eng. Ind. *92* (1970) 29.
[24] Harrison M.: J. Acoust. Soc. Am. *24* (1952) 776.
[25] Benkovskii V. G., Golubnichii P. I., Maslennikov S. I.: Akust. Zh. *20* (1974) 23.
[26] Lauterborn W.: *in* Finite-Amplitude Wave Effects in Fluids (ed. Bjørnø L.). IPC Science and Technology Press, Guildford, 1974, p. 195.
[27] Vokurka K.: Acta Tech. ČSAV *32* (1987) 162.
[28] Vokurka K.: J. Sound & Vib. *116* (1987) 483.
[29] Popov O. E., Kogarko S. M.: Fiz. Goreniya & Vzryva *12* (1976) 610.
[30] Knapp R. T., Daily J. W., Hammitt F. G.: Cavitation. McGraw-Hill, New York, 1970.